JACS
JOURNAL OF THE AMERICAN CHEMICAL SOCIETY
Article
pubs.acs.org/JACS

Enhanced Helical Folding of *ortho*-Phenylenes through the Control of Aromatic Stacking Interactions

Sanyo Mathew,[†] Laura A. Crandall,[‡] Christopher J. Ziegler,[‡] and C. Scott Hartley*[,†]

[†]Department of Chemistry & Biochemistry, Miami University, Oxford, Ohio 45056, United States
[‡]Department of Chemistry, University of Akron, Akron, Ohio 44325, United States

Supporting Information

ABSTRACT: The *ortho*-phenylenes are a simple class of foldamers, with the formation of helices driven by offset aromatic stacking interactions parallel to the helical axis. For the majority of reported *o*-phenylene oligomers, the perfectly folded conformer comprises perhaps 50−75% of the total population. Given the hundreds or thousands of possible conformers for even short oligomers, this distribution represents a substantial bias toward the folded state. However, "next-generation" *o*-phenylenes with better folding properties are needed if these structures are to be exploited as functional units within more complex architectures. Here, we report several new series of *o*-phenylene oligomers, varying both the nature and orientation of the substituents on every repeat unit. The conformational behavior was probed using a combination of NMR spectroscopy, DFT calculations, and X-ray crystallography. We find that increasing the electron-withdrawing character of the substituents gives oligomers with substantially improved folding properties. With moderately electron-withdrawing groups (acetoxy), we observe >90% of the perfectly folded conformer, and stronger electron withdrawing groups (triflate, cyano) give oligomers for which misfolded states are undetectable by NMR. The folding of these oligomers is only weakly solvent-dependent. General guidelines for the assessment of *o*-phenylene folding by NMR and UV−vis spectroscopy are also discussed.

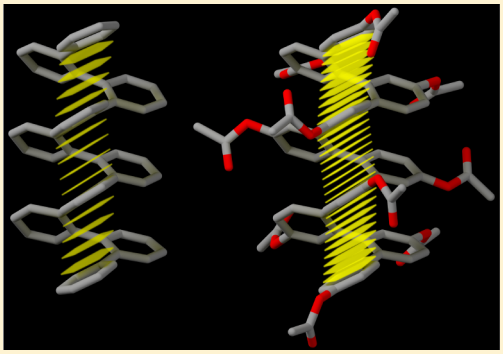

INTRODUCTION

Although largely (but not entirely[1−4]) ignored until 2010, *ortho*-phenylenes have recently been shown to fold into well-defined helices in solution, with offset stacking between every third arene repeat unit.[5−11] They are a simple, fundamental type of polyphenylene,[12] a class which now includes functional polymers,[13−15] helical oligomers and polymers,[16−18] macrocycles,[19−23] and dendrimers.[24] Understanding the folding of *o*-phenylenes is therefore important not only for their own development as foldamers[25−27] but also as models for the conformational behavior of other sterically congested polyphenylenes.[28−30] They are also beginning to be used in a variety of applications. For example, Fukushima and Aida have proposed that their folding could be exploited in chiroptical memory elements[6] and have demonstrated their use as alignment layers for discotic liquid crystals.[11] The limited conjugation along the *o*-phenylene backbone has also been used in the design of blue phosphorescent materials for LED applications.[31] Further, Ito and Nozaki have recently demonstrated a potentially transformative route to poly(*o*-arylenes) through the polymerization of aryne equivalents,[32] which could enable new applications of *o*-arylenes as helical polymers.[33]

Most of the *o*-phenylenes investigated so far are probably best described as "well-folded" in solution: while the ideal helical conformer is generally the most populated, a substantial fraction of the population is misfolded (about 25−50%), especially at the chain ends. Because for relatively long *o*-phenylene oligomers there are hundreds or thousands of possible backbone conformations, this behavior represents a substantial bias toward folding. Clearly, however, future exploitation of *o*-phenylenes will require structures with improved folding behavior. To this end, Fukushima and Aida recently reported a series of *o*-phenylene oligomers that exhibit a much higher proportion of perfect folding because of a steric effect of terminal substituents.[10] Remarkably, this effect is strongly solvent-dependent, with excellent folding in acetonitrile but a broad distribution of other conformers in other solvents (chloroform, toluene, DMF, and DMSO), as observed by NMR spectroscopy. To the best of our knowledge, the specific mechanism of this solvent-dependence has not yet been determined. Regardless, the improved folding of these compounds was shown to significantly impact their basic properties, specifically their UV−vis absorption and electrochemical behavior. There is, however, still no general design strategy for *o*-phenylenes that fold perfectly (or near-perfectly) under a variety of conditions.

We recently reported a simple model to explain the folding behavior of *o*-phenylenes.[9] Briefly, the relative stability of *o*-phenylene conformers obeys two simple rules: (1) a specific sequence of biaryl torsional angles is prohibited because of

Received: September 25, 2014
Published: November 6, 2014

   dx.doi.org/10.1021/ja509902m | J. Am. Chem. Soc. 2014, 136, 16666−16675

steric strain (so-called "ABA" sequences; see below), and (2) conformer stability is otherwise a simple function of the number of (offset) aromatic stacking interactions possible for the geometry. In essence, the folding of *o*-phenylenes can be understood by analogy with α-helices, with aromatic stacking interactions in place of hydrogen bonding. We found that, for the parent (unsubstituted) *o*-phenylene, these interactions each account for about $\Delta G^\circ \approx -0.5$ kcal/mol. This model can be used for semiquantitative predictions of oligomer folding propensities. For example, unsubstituted poly(*o*-phenylene) ought not to be particularly well-folded, consistent with the experimental behavior of short oligomers.[8] However, relatively small increases in the strength of the arene−arene interactions (to $\Delta G^\circ \approx -1$ to -2 kcal/mol) are predicted to substantially improve the folding behavior.

One approach to enhance the folding of *o*-phenylenes would be to supplement arene−arene stacking with additional interactions along the helix (e.g., H-bonding). However, an attractive strategy would be to control the conformational behavior through substituent effects on the aromatic stacking interactions themselves. Here, we report the synthesis of several new series of substituted *o*-phenylene oligomers with two different substitution patterns, $\mathbf{oP}^n(\mathbf{X})_n{}^{\mathbf{A}}$ and $\mathbf{oP}^n(\mathbf{X})_n{}^{\mathbf{B}}$, shown in Chart 1. These oligomers are conveniently prepared through

Chart 1

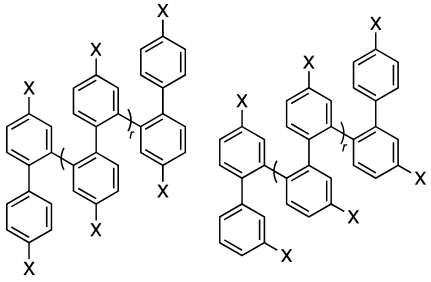

a divergent, postoligomerization modification strategy. We find that the substituents (X) have a substantial effect on the folding properties of the oligomers. By increasing their electron-withdrawing character, it is possible to achieve near-perfect folding (as judged by NMR) through the strengthening of aromatic stacking. Importantly, good folding is observed in a variety of different solvents, and this behavior is observed for substituents (e.g., simple esters) that will provide convenient points of attachment for future applications requiring functionalization of the oligomers. This design strategy should also be readily applied to the control of the folding behavior of other classes of polyphenylenes.

RESULTS AND DISCUSSION

Oligomer Design. A long-term goal of this project (and for foldamers more generally[27]) is to incorporate abiotic foldamer subunits, with their well-defined secondary structures, into more complex, functional, three-dimensional architectures. *o*-Phenylenes should be well-suited to this challenge because of their structural simplicity, their simple folding mechanism, and the wide array of synthetic methods developed for the functionalization of arenes. Implicit in this goal is the need to control the location of functionality on the exterior of the *o*-phenylene helix. Thus, as part of this study we wished to evaluate not only how the nature of the substituents affects the folding behavior but also their position. For the isomeric $\mathbf{oP}^n(\mathbf{X})_n{}^{\mathbf{A}}$ and $\mathbf{oP}^n(\mathbf{X})_n{}^{\mathbf{B}}$ series, the substituents are oriented very differently when the oligomers are folded into stacked helices. As shown in Figure 1, in the A-series the substituents

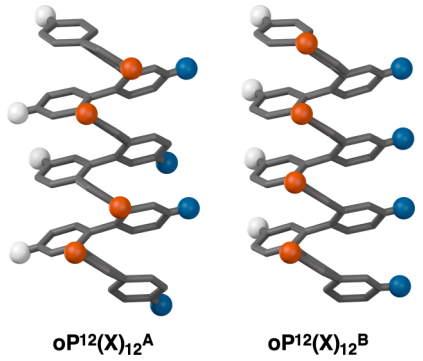

Figure 1. Substituent alignment in $\mathbf{oP}^{12}(\mathbf{X})_{12}{}^{\mathbf{A}}$ and $\mathbf{oP}^{12}(\mathbf{X})_{12}{}^{\mathbf{B}}$ when perfectly folded. The spheres represent substituent (X) positions and are colored according to particular stacks of repeat units. The hydrogen atoms have been removed for clarity.

will assume a zig−zag pattern, with two characteristic distances of roughly 3.4 and 5.3 Å between them.[34] Alternatively, in the B-series, the substituents will assume a directly eclipsed, stacked orientation with a constant spacing of 3.6 Å. In both cases, the substituents on adjacent rings are in very close proximity, which is known to have a substantial impact on substituent effects in aromatic stacking interactions.[35]

Synthesis. The synthesis of the $\mathbf{oP}^n(\mathbf{OMe})_n{}^{\mathbf{A}}$ series has already been reported.[5] The new $\mathbf{oP}^n(\mathbf{OMe})_n{}^{\mathbf{B}}$ series required a slight modification of the original synthetic approach through a new 9,10-boroxarophenanthrene monomer **3** (Scheme 1).

Scheme 1. Synthesis of Key Monomer 3 [a]

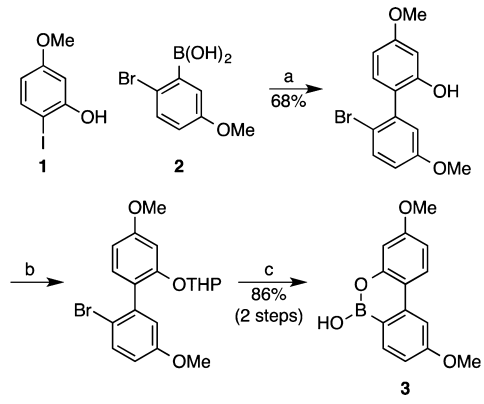

[a]Reagents and conditions: (a) $Pd(PPh_3)_4$, K_2CO_3(aq), toluene/EtOH, Δ; (b) dihydropyran, PPTS, CH_2Cl_2; (c) (i) ^{n}BuLi, THF, −70 °C, (ii) $B(O^iPr)_3$, (iii) HCl(aq).

These monomers are conveniently used in monodisperse *o*-phenylene synthesis, as Suzuki coupling unmasks a hydroxyl group which can be used for further coupling steps following triflation (this strategy is based on Manabe's polyphenylene synthesis[36]). As shown in Scheme 1, compound **3** was synthesized by Suzuki coupling of known 2-iodo-5-methoxyphenol **1**[37] and 2-bromo-5-methoxyphenylboronic acid **2**[38]

dx.doi.org/10.1021/ja509902m | J. Am. Chem. Soc. 2014, 136, 16666−16675

followed by protection of the hydroxyl group with THP, metal–halogen exchange, and boronation. Cyclization to **3** occurred spontaneously on hydrolysis of the THP group and boronate ester.

The oligomer synthesis of the $\mathbf{oP^{\mathit{n}}(OMe)_{\mathit{n}}}^{\mathbf{B}}$ series is shown in Scheme 2. Briefly, monomer **3** was coupled with 3-

Scheme 2. Synthesis of Oligomers $\mathbf{oP^{\mathit{n}}(OMe)_{\mathit{n}}}^{\mathbf{B}}$ [a]

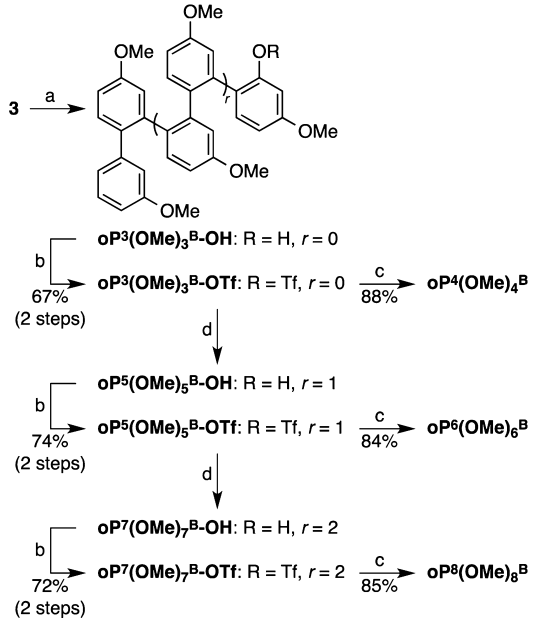

[a]Reagents and conditions: (a) 3-iodoanisole, $Pd(OAc)_2$, SPhos, K_3PO_4, THF/H_2O, Δ; (b) Tf_2O, pyridine, CH_2Cl_2; (c) 4-methoxyphenylboronic acid, $Pd(OAc)_2$, SPhos, K_3PO_4, THF/H_2O, Δ; (d) **3**, $Pd(OAc)_2$, SPhos, K_3PO_4, THF/H_2O, Δ.

iodoanisole. The resulting hydroxyl-terminated oligomer $\mathbf{oP^3(OMe)_3}^{\mathbf{B}}$**-OH** was then triflated to give $\mathbf{oP^3(OMe)_3}^{\mathbf{B}}$**-OTf**. This intermediate could then be capped by coupling to 4-methoxyphenylboronic acid, or oligomer growth could be continued by coupling to an additional equivalent of **3**. In principle, this sequence could be repeated indefinitely to prepare higher oligomers; for this study we chose to stop at the octamer $\mathbf{oP^8(OMe)_8}^{\mathbf{B}}$.

With both sets of methoxy-substituted oligomers in hand, we then proceeded to develop conditions for their refunctionalization. This postoligomerization modification highlights one of the more useful aspects of the *o*-phenylene backbone: because it is structurally very simple, it is largely inert to a wide variety of conditions that can be used for substituent functional group interconversion.[39] As shown in Scheme 3, deprotection of the methoxy groups with BBr_3 gave oligomers $\mathbf{oP^{\mathit{n}}(OH)_{\mathit{n}}}$ in good yields. These hydroxyl-substituted compounds gave broadened, complex NMR spectra, presumably because of the added effect of hydrogen bonding on their conformational distributions. They were therefore carried through to the next steps without complete characterization. Esterification of $\mathbf{oP^{\mathit{n}}(OH)_{\mathit{n}}}$ was accomplished with acetic anhydride to afford $\mathbf{oP^{\mathit{n}}(OAc)_{\mathit{n}}}$ in good yields. Similarly, triflation was accomplished with triflic anhydride to give oligomers $\mathbf{oP^{\mathit{n}}(OTf)_{\mathit{n}}}$. These triflated oligomers obviously have significant potential for further functionalization through transition-metal-catalyzed coupling reactions. An exploration of such derivatives is beyond the scope of this study. However, the triflates did provide a

Scheme 3. Refunctionalization of Methoxy-Substituted *o*-Phenylenes [a]

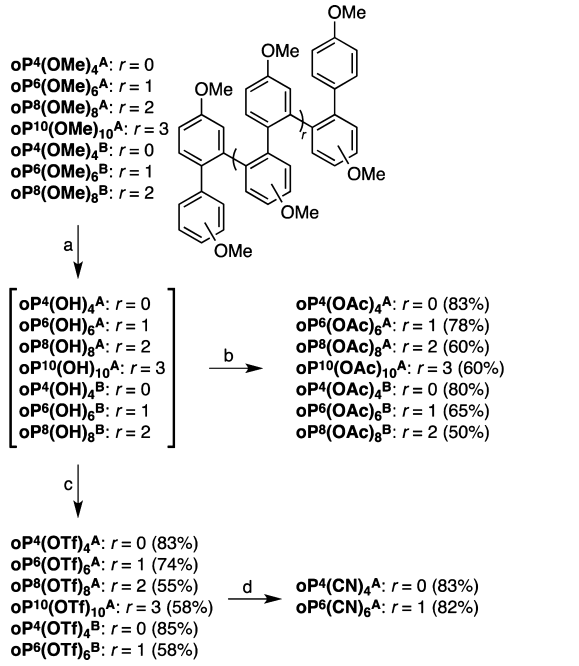

[a]Reagents and conditions: (a) BBr_3, CH_2Cl_2, −78 °C to rt; (b) Ac_2O, NEt_3, CH_2Cl_2, 40 °C; (c) Tf_2O, pyridine, CH_2Cl_2, 0 °C to rt; (d) $Zn(CN)_2$, $Pd(PPh_3)_4$, DMF, 120 °C.

convenient platform for cyanation with $Zn(CN)_2$ and catalytic $Pd(PPh_3)_4$ to give $\mathbf{oP^{\mathit{n}}(CN)_{\mathit{n}}}^{\mathbf{A}}$ (n = 4, 6). Unfortunately, attempts to cyanate $\mathbf{oP^6(OTf)_6}^{\mathbf{B}}$ gave intractable mixtures from which $\mathbf{oP^6(CN)_6}^{\mathbf{B}}$ could not be adequately purified. Cyanation of the higher oligomers was attempted, but poor solubility precluded the isolation and purification of the products.

X-ray-quality crystals were obtained for four of the oligomers: $\mathbf{oP^6(OMe)_6}^{\mathbf{B}}$ (CH_2Cl_2/hexanes), $\mathbf{oP^8(OTf)_8}^{\mathbf{A}}$ (CH_2Cl_2/hexanes), $\mathbf{oP^{10}(OAc)_{10}}^{\mathbf{A}}$ (CH_2Cl_2/hexanes), and $\mathbf{oP^{10}(OTf)_{10}}^{\mathbf{A}}$ (CH_2Cl_2/hexanes/ethanol), with the resulting structures shown in Figure 2. In three of the four cases, the compounds crystallize as racemates ($P\bar{1}$ space group). Compound $\mathbf{oP^8(OTf)_8}^{\mathbf{A}}$ crystallizes as a conglomerate ($P2_12_12_1$). Although there is some disorder in the orientation of the side chains (particularly for $\mathbf{oP^{10}(OTf)_{10}}^{\mathbf{A}}$), in all cases the *o*-phenylene backbones are folded into helical, stacked conformations ("A_{n-3}" conformations, as discussed below). While these solid-state structures do not unambiguously establish the solution-phase folding behavior of the compounds (e.g., because of crystal packing forces),[5,7] they do confirm that these oligomers are able to fold well despite the presence of sterically demanding substituents (acetoxy and especially triflate). To the best of our knowledge, the decamers reported here are the longest *o*-phenylenes characterized crystallographically to this point (Fukushima and Aida have previously reported the crystal structure of an octamer,[6] and there are now many examples of hexamers[4,5,9,10]).

Conformational Analysis of $\mathbf{oP^6(X)_6}$. We have discussed the conformational behavior of the *o*-phenylenes in detail previously.[7,9] Briefly, the backbone conformation of an *o*-phenylene is dictated by the biaryl dihedral angles φ_i, as shown in Figure 3. For a typical *o*-phenylene, each φ_i can assume one of four values: $\varphi_i \approx \pm 55°$ or $\pm 130°$. However, rotation about

dx.doi.org/10.1021/ja509902m | J. Am. Chem. Soc. 2014, 136, 16666−16675

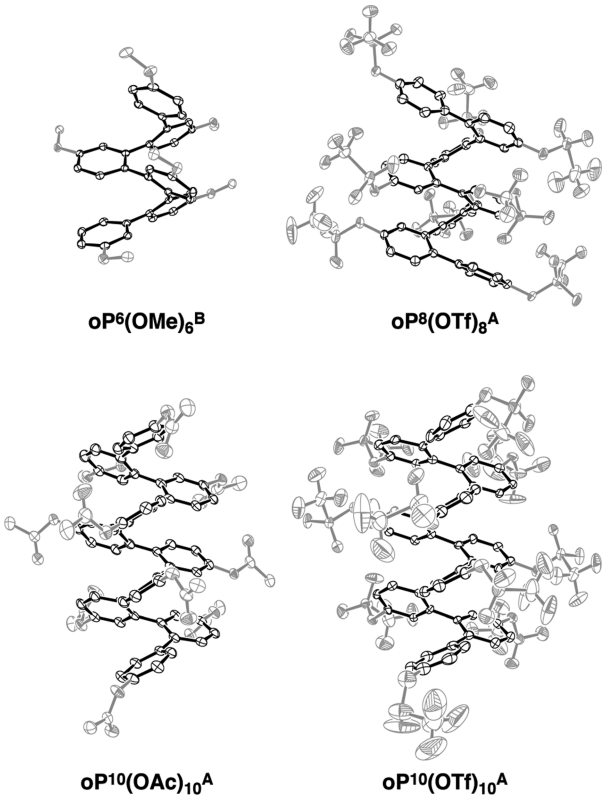

Figure 2. Solid-state structures of $\mathbf{oP^6(OMe)_6}^{\mathbf{B}}$, $\mathbf{oP^8(OTf)_8}^{\mathbf{A}}$, $\mathbf{oP^{10}(OAc)_{10}}^{\mathbf{A}}$, and $\mathbf{oP^{10}(OTf)_{10}}^{\mathbf{A}}$. For clarity, the hydrogen atoms have been omitted and the side chains are depicted in gray. One of the OTf groups in $\mathbf{oP^{10}(OTf)_{10}}^{\mathbf{A}}$ is disordered; only one possible orientation is shown here.

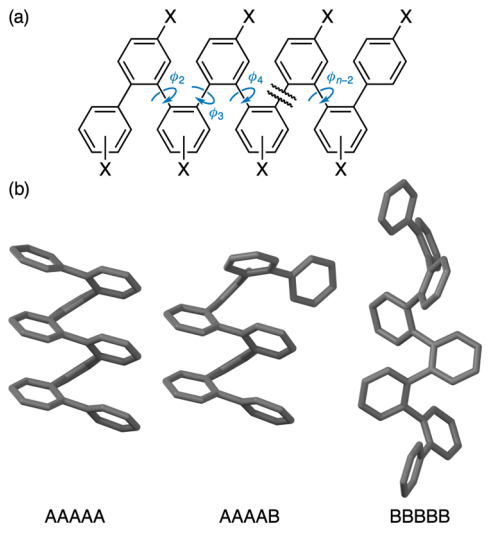

Figure 3. (a) Backbone dihedral angles controlling the folding of an *o*-phenylene. (b) Representative conformers for $\mathbf{oP^8(H)_8}$.

the various bonds is coupled: within a single (short) molecule, only two φ_i values can coexist, either −55°/+130° (A/B) or +55°/−130° (A′/B′),[7] giving two conformational populations that are enantiomeric. Specific folding states can be described using a simple binary notation (i.e., ABA... or A′B′A′...). The AA...A (A_{n-3}) conformers represent the perfectly folded helical states with offset aromatic stacking. This state typically predominates for simple *o*-phenylenes; the solid-state structures in Figure 2 are all A_{n-3} conformers. Misfolding is typically manifested as B states localized at the ends of the oligomer strand (φ_2 or φ_{n-2}), for reasons that we have discussed previously.[9] In other words, the AA...B state is the second-most populated conformational state for typical *o*-phenylene oligomers, which can therefore be thought of as helices with "frayed ends". The other extreme, the BB...B (B_{n-3}) conformers, are extended helices without aromatic stacking. These conformers have been demonstrated for some architectures related to *o*-phenylenes, in particular many examples of sterically hindered poly(2,3-quinoxalines).[40,41]

An important feature of the *o*-phenylenes is that the interconversion between these different backbone conformers is slow on the NMR time scale (for oligomers longer than the pentamer). Thus, a typical NMR spectrum of an *o*-phenylene oligomer is comprised of contributions from various conformational states. While this phenomenon greatly complicates routine characterization, it also provides an important means to quantify the folding state of the oligomer. It is possible to assign the ^{1}H chemical shifts of the different conformations using standard two-dimensional NMR techniques. In general, these chemical shifts are highly sensitive to the oligomer's geometry because different conformers orient protons differently with respect to the shielding zones of nearby aromatic rings, resulting in changes of up to $\Delta\delta \approx 2$ ppm. These chemical shift changes are readily predicted using DFT calculations;[7] thus, specific backbone geometries can be assigned to the experimental data. The relative populations of different conformers can then be determined by integration (or deconvolution of overlapping peaks).

We began by focusing on the behavior of the substituted *o*-phenylene hexamers in chloroform-*d* at 268 K.[42] For each oligomer, complete sets of ^{1}H and ^{13}C chemical shifts were obtained for the most prominent conformer from COSY, HMQC, and HMBC spectra. This major conformer was always 2-fold symmetric. In all cases, the smaller signals in the spectra, when observed, were confirmed to arise from minor conformational states (as opposed to impurities) using EXSY (i.e., NOESY) spectroscopy, which gave clear cross-peaks that were in phase with the diagonal (indicating chemical exchange as opposed to through-space interactions). The EXSY spectrum of $\mathbf{oP^6(OMe)_6}^{\mathbf{B}}$ is shown in Figure 4 as a representative example.

Assigning the experimental data to specific folding states requires computational geometries that can be used for comparison. Unfortunately, these new oligomers are much more structurally complex than those we have previously examined: the methoxy, acetoxy, and especially triflate substituents can assume many possible orientations, which have a significant effect on the chemical shifts of nearby protons. It was not possible to separately optimize every possible conformation. Instead, we generated a library of substituent orientations using the MMFF molecular mechanics method, optimized the best 200 candidates using the PM7 semiempirical method,[43] and then carried out single-point PCM/B97-D/TZV(2d,2p) calculations.[44] The lowest-energy conformer was chosen for full optimization (see the Supporting Information). While this strategy is unlikely to provide the exact global energy minimum, it provides geometries of sufficient quality for NMR prediction. Thus, the AAA, AAB, and BBB backbone geometries were optimized for all of the hexamers. ^{1}H isotropic shieldings were calculated for each of the geometries at the PCM/WP04/6-31G(d) level,[45] which has been shown to provide high-quality NMR predictions for a

dx.doi.org/10.1021/ja509902m | J. Am. Chem. Soc. 2014, 136, 16666−16675

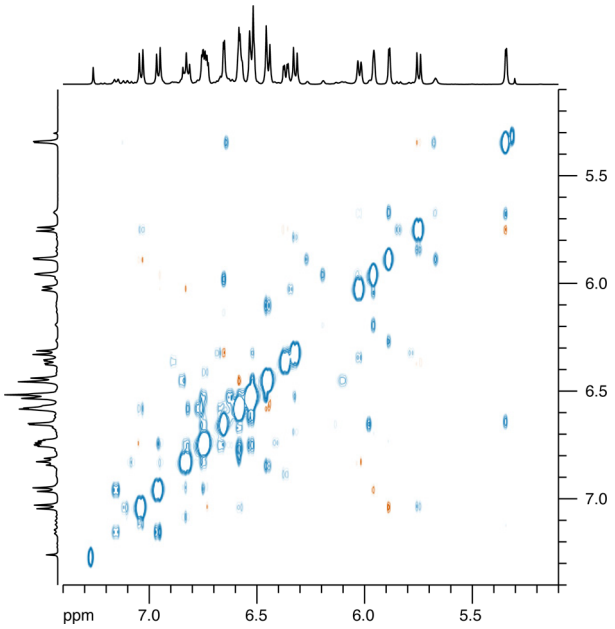

Figure 4. EXSY spectrum (500 MHz, 268 K, $CDCl_3$) of $\mathbf{oP^6(OMe)_6}^{\mathbf{B}}$.

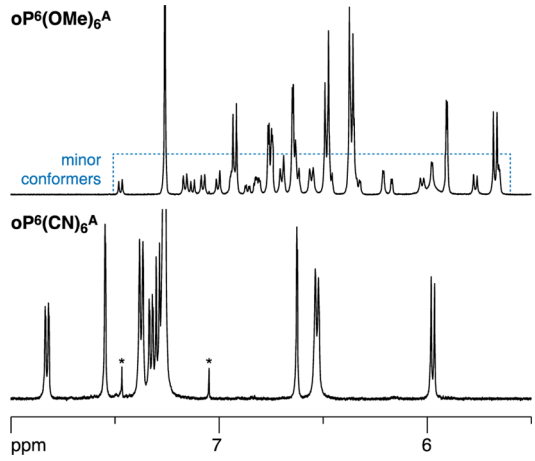

Figure 5. ^{1}H NMR spectra (500 MHz, 268 K, $CDCl_3$) of representative *o*-phenylene hexamers $\mathbf{oP^6(OMe)_6}^{\mathbf{A}}$ and $\mathbf{oP^6(CN)_6}^{\mathbf{A}}$ (aromatic regions). The peaks labeled * are the ^{13}C isotopic side bands from residual $CHCl_3$.

variety of organic molecules[46] and which has worked well for *o*-phenylenes in the past.[47] The experimental chemical shift assignments were then compared to the computational data. In all cases, the perfectly folded AAA geometries provide the best match to the experimental data, with RMS errors <0.25 ppm. In some cases, the errors are slightly higher than the thresholds we have previously used for *o*-phenylenes (~0.15 ppm). However, the protons exhibiting the largest deviations from the experimental chemical shifts are typically located close to the substituents (e.g., in the deshielding zone of an acetate group). Thus, these poorer matches likely result from our inability to fully account for the substituent orientations. The quality of the matches was analyzed statistically (see Supporting Information); for all of the hexamers, the AAA geometries are the best matches to the major conformer observed experimentally with a high degree of confidence ($p \leq 0.016$).

The ^{1}H NMR spectrum of the previously reported $\mathbf{oP^6(OMe)_6}^{\mathbf{A}}$ at 268 K, shown in Figure 5 (top), is typical of the *o*-phenylenes we (and others) have examined to this point. The occurrence of minor conformational states is readily apparent from the small signals in the spectrum. As discussed above, it is straightforward to determine the fraction of molecules that are "perfectly folded" (i.e., in the AAA state) by integration. The most prominent set of signals can be assigned to the AAA conformer (67% of the population for $\mathbf{oP^6(OMe)_6}^{\mathbf{A}}$); however, there are also significant minor signals arising from the AAB (24%) and BAB (9%) conformers. Similar behavior is observed for the parent oligomer $\mathbf{oP^6(H)_6}$ (49:42:9 AAA:AAB:BAB). In contrast, many of the new compounds exhibit substantially improved folding behavior. Oligomer $\mathbf{oP^6(CN)_6}^{\mathbf{A}}$ exhibits no evidence of any minor conformers at all, as shown in Figure 5 (bottom). In principle, the simplified ^{1}H NMR spectrum could also indicate a transition to rapid conformational exchange. This explanation is unlikely, however, given the excellent match to the DFT calculations for the perfectly folded conformer. We also observed further slowing of biaryl bond rotation for one of the oligomers ($\mathbf{oP^6(OTf)_6}^{\mathbf{A}}$), as discussed below.

The AAA conformer populations for all eight *o*-phenylene hexamers are compiled in Table 1, along with ΔG°_{fold} values

Table 1. AAA Conformer Populations for the *o*-Phenylene Hexamers at 268 K and Associated ΔG°_{fold} and ΔE_{tet} Values[a]

compound	σ_m	%AAA	ΔG°_{fold} (kcal/mol)[a]	ΔE_{tet} (kcal/mol)
$\mathbf{oP^6(H)_6}$	0.00	49%	+0.02 ± 0.08	−2.1
$\mathbf{oP^6(OMe)_6}^{\mathbf{A}}$	0.12	67%	−0.38 ± 0.08	−2.6
$\mathbf{oP^6(OAc)_6}^{\mathbf{A}}$	0.39	93%	−1.38 ± 0.08	−4.4
$\mathbf{oP^6(OTf)_6}^{\mathbf{A}}$	0.56	94%	−1.47 ± 0.08	−4.8
$\mathbf{oP^6(CN)_6}^{\mathbf{A}}$	0.56	>96%	<−1.69 ± 0.08	−3.3
$\mathbf{oP^6(OMe)_6}^{\mathbf{B}}$	0.12	89%	−1.11 ± 0.08	−3.0
$\mathbf{oP^6(OAc)_6}^{\mathbf{B}}$	0.39	81%	−0.77 ± 0.08	−4.5
$\mathbf{oP^6(OTf)_6}^{\mathbf{B}}$	0.56	88%	−1.06 ± 0.08	−3.2

[a]Errors calculated assuming ±10% errors on the ^{1}H NMR integrations.

corresponding to the reaction [all unfolded conformers] ⇌ AAA.[48] Clearly, both the nature and position of the substituents have significant effects on the folding of the oligomers. Indeed, most of the new *o*-phenylenes reported here have dramatically improved folding propensities compared to those previously reported, with >90% of the population in the AAA geometry.

In general terms, improved folding is observed with increasingly electron-withdrawing substituents. This is particularly evident in the $\mathbf{oP^6(X)_6}^{\mathbf{A}}$ series, where the substituents are slightly offset in the folded conformation (Figure 1). A plot of ΔG°_{fold} against the Hammett constant[49] σ_m is shown in Figure 6. Because we can only establish an upper bound for its value, the folding energy of $\mathbf{oP^6(CN)_6}^{\mathbf{A}}$ is shown on the plot but was excluded from linear regression. A good, statistically significant correlation is observed for the remaining data, with $r = -0.97$ ($p = 0.03$). The quality of the correlation with σ_m is typical of systems designed to quantify arene−arene interactions, including molecular torsion balances and related systems.[50−52] It is also consistent with the behavior we previously observed for singly substituted *o*-phenylenes.[9] This result, therefore, strongly implies that it is the effect of the substituents on the aromatic stacking interactions that ultimately controls the folding propensity.

dx.doi.org/10.1021/ja509902m | J. Am. Chem. Soc. 2014, 136, 16666−16675

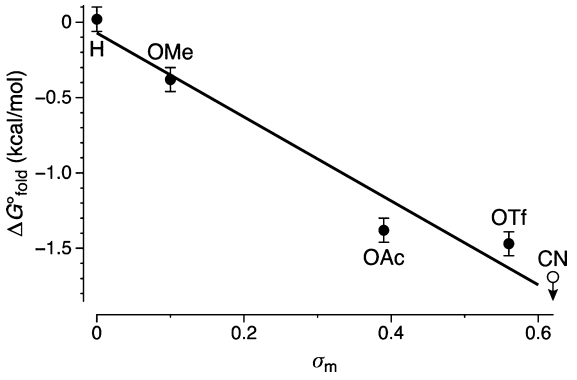

Figure 6. ΔG°_{fold} plotted against σ_m for the $\mathbf{oP^6(X)_6^A}$ series. The point for $\mathbf{oP^6(CN)_6^A}$ represents the upper limit on ΔG°_{fold} and is not included in the regression.

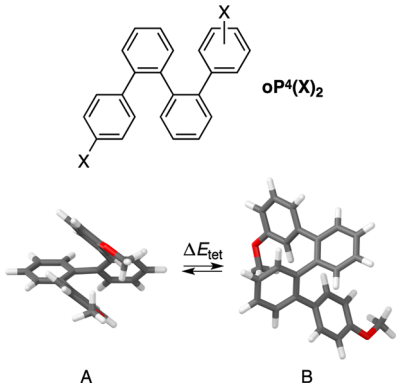

Figure 7. Conformational energy difference considered for model compounds $\mathbf{oP^4(X)_2}$, with the optimized geometries of $\mathbf{oP^4(OMe)_2^B}$ shown as a representative example. The orientations of the *meta*-substituted ring in the two states have been chosen such that they represent the orientations when buried within a longer oligomer.

Conversely, no significant correlation is observed between σ_m and ΔG°_{fold} for the $\mathbf{oP^6(X)_6^B}$ series, as shown in the Supporting Information. For this series, the substituents are eclipsed when folded (Figure 1). Recent work by Wheeler on the cofacial stacking of substituted arenes has shown that substituent–substituent effects dominate the energies of arene dimers when the substituents are in close proximity.[35] Similar results for parallel-displaced stacks suggests that the correlation between dimerization energy and electron-withdrawing power of the substituents breaks down for stacks analogous to $\mathbf{oP^n(X)_n^B}$.[53] From comparison of the isomeric A- and B-series *o*-phenylene hexamers, it is likely that a combination of steric effects and electrostatic repulsion act to decrease the folding ability of the acetoxy- and triflate-substituted compounds. Interestingly, however, the interactions between directly stacked substituents are not always unfavorable, as $\mathbf{oP^6(OMe)_6^B}$ exhibits improved folding properties compared to $\mathbf{oP^6(OMe)_6^A}$.

Some additional insight into the substituent effects can be obtained through DFT calculations at the PCM/B97-D/TZV(2d,2p) level. In previous work, we showed that similar calculations effectively model the effect of substituents on the folding of terminally substituted *o*-phenylene hexamers.[9] However, the increased complexity of the substituents used here precludes direct analysis of the hexamers themselves because of the thousands of possible substituent orientations for the acetoxy- and triflate-substituted oligomers: unfortunately, changes in substituent orientations give changes in the calculated energy that are comparable to the energy differences between the backbone conformers themselves.

To simplify the system, we instead considered the energy differences ΔE_{tet} between the A and B conformers of tetramers $\mathbf{oP^4(X)_2}$, shown in Figure 7. While this is obviously a gross structural simplification, this model system allows us to probe substituent effects on the stacking interactions while also capturing the conformational constraints imposed by the *o*-phenylene structure. As there are only two substituents per structure, it was possible to explicitly optimize all possible[54] starting side-chain conformations for both backbone geometries. For the $\mathbf{oP^4(X)_2^B}$ series, the *meta*-substituted ring can be oriented in two different directions; only the orientation that directly corresponds to folding within a longer *o*-phenylene was considered (i.e., with the substituent pointed away from the helical path; see Figure 7). The ΔE_{tet} values are the energy differences between the most-stable substituent conformations that were identified for the A and B conformers and are included in Table 1.

The experimental ΔG°_{fold} show a reasonable correlation with ΔE_{tet}, as shown in the Supporting Information, with one notable exception: the folding energy of $\mathbf{oP^6(CN)_6^A}$ is significantly underestimated. The calculations are also better at predicting the folding of the A-series hexamers than the B-series. Nevertheless, the calculated energies on the $\mathbf{oP^4(X)_2}$ model systems are in agreement with the experimental behavior in several key ways: First, the calculations correctly predict that all substituents give improved folding relative to the parent $\mathbf{oP^6(H)_6}$. Second, with the exception of the $\mathbf{oP^6(CN)_6^A}$, the calculated energies are broadly consistent with the observation that increased electron-withdrawing power (as measured through σ_m) gives better folding. Third, for the methoxy- and triflate-substituted oligomers, the DFT calculations correctly predict the effect of switching from the A-series to the B-series substitution patterns. Notably, this effect occurs in opposite directions in these two cases, with better folding in $\mathbf{oP^6(OMe)_6^B}$ vs $\mathbf{oP^6(OMe)_6^A}$ but worsened folding for $\mathbf{oP^6(OTf)_6^B}$ vs $\mathbf{oP^6(OTf)_6^A}$. For the acetate-substituted oligomers, the model system predicts essentially the same folding energy regardless of the position of the substituent. While the prediction is wrong, the discrepancy is small considering the simplification of the model system and its treatment of the substituents as static groups.

Broadly speaking, the calculations on $\mathbf{oP^4(X)_2}$ are consistent with the behavior we observe experimentally and parallel previous work on arene stacking in *o*-phenylenes,[9] supporting the idea that it is a substituent's effect on aromatic stacking interactions that is ultimately responsible for differences in folding. However, as a predictive tool, this model system is not substantially better than simply referring to σ_m values.

Further support for the enhancement of stacking interactions with electron-withdrawing substituents comes from the variable-temperature ^{1}H NMR of $\mathbf{oP^6(OTf)_6^A}$ in chloroform-*d*. While running the experiments at 268 K, we observed a slight broadening of two signals, associated with the protons on the (*para*-substituted) terminal rings, that was not found for any of the other hexamers. Upon further cooling, these two signals continue to broaden and then separate into two signals each, as shown in Figure 8 (unfortunately, the signals do not then sharpen above the freezing point of chloroform-*d*). The other signals are essentially unchanged over this same temperature range. We interpret this behavior as slowing rotation about the

dx.doi.org/10.1021/ja509902m | J. Am. Chem. Soc. 2014, 136, 16666−16675

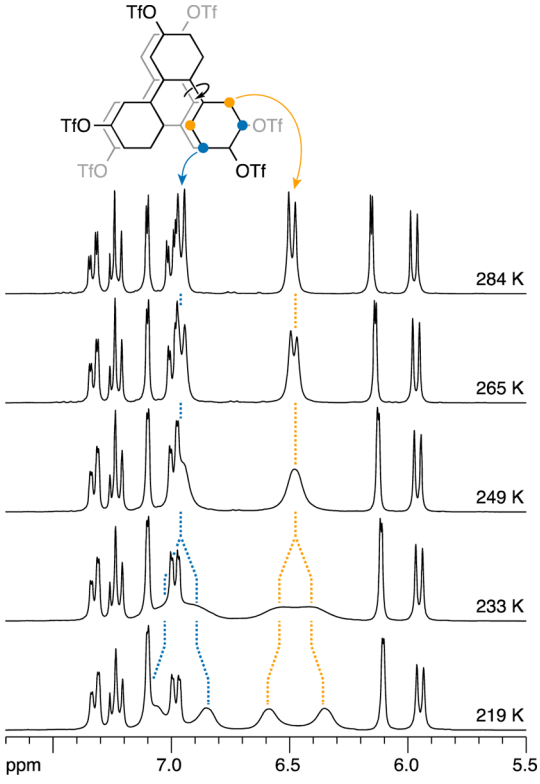

Figure 8. Low-temperature ^{1}H NMR of $\mathbf{oP^6(OTf)_6}^{\mathbf{A}}$ ($CDCl_3$, 300 MHz). Rotation about φ_1 (or φ_5) is indicated on the structure.

terminal biaryl bonds with decreasing temperature (φ_1/φ_5, Figure 3a), implying that the triflate groups, among the best in terms of folding enhancement, substantially increase the strength of the stacking interactions between these terminal rings and the rest of the oligomer. This result also confirms that the spectral simplification observed for the triflate- and cyano-substituted oligomers does not result from a switch to rapid conformational exchange.

Longer Oligomers. The folding properties of $\mathbf{oP^8(H)_8}$, $\mathbf{oP^8(OMe)_8}^{\mathbf{A}}$, and $\mathbf{oP^{10}(OMe)_{10}}^{\mathbf{A}}$ have already been reported.[5,8] The new oligomers $\mathbf{oP^8(OMe)_8}^{\mathbf{B}}$, $\mathbf{oP^8(OAc)_8}^{\mathbf{A}}$, $\mathbf{oP^{10}(OAc)_{10}}^{\mathbf{A}}$, $\mathbf{oP^8(OAc)_8}^{\mathbf{B}}$, $\mathbf{oP^8(OTf)_8}^{\mathbf{A}}$, and $\mathbf{oP^{10}(OTf)_{10}}^{\mathbf{A}}$ were studied by NMR spectroscopy using the same approach as that for the hexamers. In each case, the ^{1}H and ^{13}C chemical shifts for the most prominent conformer were extracted from 2D NMR spectra. Minor signals (when observable) were confirmed to arise from other conformational states by the observation of cross-peaks in the EXSY spectra. It was not possible to explicitly assign these minor signals, as they were typically too weak (see below).

To confirm that for each oligomer the major species in solution is the perfectly folded helix, geometries of the AA...A, AA...B, and BB...B conformers were obtained at the B3LYP/6-31G(d) level, with the substituents oriented according to an MMFF conformational search for the AA...A conformer. This level of theory does not accurately capture the energetics of *o*-phenylene folding; however, we have previously shown that the backbone geometries are adequate for comparison with the NMR data.[7] As for the hexamers, the AA...A geometries are the best matches to the experimental NMR data in all cases. These matches can be made with a high degree of statistical confidence for most of the new oligomers ($p \leq 0.02$). The acetate substituents again have a strong, orientation-dependent effect on the chemical shifts which is difficult to capture in a single geometry. The RMS errors are relatively large (>0.2 ppm) for $\mathbf{oP^8(OAc)_8}^{\mathbf{A}}$ and $\mathbf{oP^{10}(OAc)_{10}}^{\mathbf{A}}$, and the statistical confidence that the perfectly folded conformer is the best match is weaker ($p > 0.09$). Nevertheless, given the reasonable RMS errors, the parallels with the other oligomers, and that the A_7 geometry is observed in the solid state for $\mathbf{oP^{10}(OAc)_{10}}^{\mathbf{A}}$, we conclude that these acetate-substituted oligomers are also predominantly in the AA...A state.

On inspection of the ^{1}H NMR spectra, it is immediately apparent that the folding of these new oligomers is dramatically improved compared to other examples in the literature, as shown in Figure 9 for $\mathbf{oP^{10}(OAc)_{10}}^{\mathbf{A}}$ and $\mathbf{oP^{10}(OTf)_{10}}^{\mathbf{A}}$

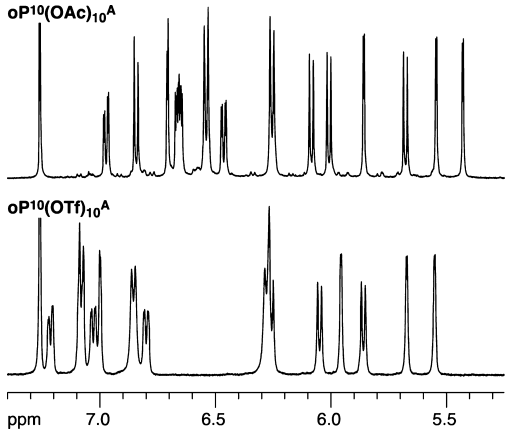

Figure 9. Representative ^{1}H NMR spectra (500 MHz, $CDCl_3$, rt) of longer *o*-phenylene oligomers $\mathbf{oP^{10}(OAc)_{10}}^{\mathbf{A}}$ and $\mathbf{oP^{10}(OTf)_{10}}^{\mathbf{A}}$ (aromatic region).

(compare to the spectrum of $\mathbf{oP^6(OMe)_6}^{\mathbf{B}}$ in Figure 5). Indeed, for the longer triflate-substituted oligomers, $\mathbf{oP^8(OTf)_8}^{\mathbf{A}}$ and $\mathbf{oP^{10}(OTf)_{10}}^{\mathbf{A}}$, there is no indication of minor conformational states at all. Unfortunately, the folding of the new octamers and decamers is much more difficult to quantify than that of the hexamers (Table 1). Essentially, they fold too well: the signals from the minor conformational states are too weak, and without specific assignments we cannot definitively determine the population distribution by integration. This problem is exacerbated in the less-symmetrical B-series oligomers. However, it is clear that the substituent effects observed for the hexamers hold in these more complex systems: The folding of $\mathbf{oP^8(OMe)_8}^{\mathbf{B}}$ is about 2-fold better than that of $\mathbf{oP^8(OMe)_8}^{\mathbf{A}}$. Both $\mathbf{oP^8(OAc)_8}^{\mathbf{A}}$ and $\mathbf{oP^{10}(OAc)_{10}}^{\mathbf{A}}$ exhibit >90% of the perfectly folded AA...A conformer at equilibrium, whereas the folding of $\mathbf{oP^8(OAc)_8}^{\mathbf{B}}$ is noticeably worse. Likewise, $\mathbf{oP^8(OTf)_8}^{\mathbf{A}}$ and $\mathbf{oP^{10}(OTf)_{10}}^{\mathbf{A}}$ exhibit essentially perfect folding, with no indication of minor conformational states at all. Compared to $\mathbf{oP^{10}(OMe)_{10}}^{\mathbf{A}}$, for which only about 50% of the population is in the A_7 state, all of the acetoxy- and triflate-substituted oligomers give substantially improved folding.

As mentioned in the introduction, Fukushima and Aida recently reported oligomers of general structure $\mathbf{oP^n(FA)}$, shown in Chart 2, which show much improved folding when dissolved in acetonitrile, but not other solvents, because of a steric effect at the oligomer ends.[10] While not explicitly reported, the folding of these *o*-phenylenes appears to be comparable to that of the $\mathbf{oP^n(OAc)_n}^{\mathbf{A}}$ series in chloroform-*d* (i.e., the NMR spectra are dominated by peaks associated with

dx.doi.org/10.1021/ja509902m | J. Am. Chem. Soc. 2014, 136, 16666−16675

Chart 2

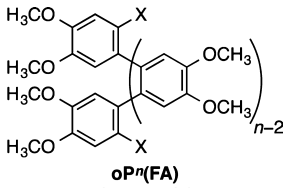

the major conformer, but contributions from minor conformational states are observable). Thus, the strategy reported here—improved folding through enhancement of aromatic stacking interactions—gives oligomers that show even better folding than the previous best case of **oP^n(FA)** in acetonitrile (**oP^n(OTf)$_n$**^{A} and **oP^6(CN)$_6$**^{A} in chloroform). Of course, the two strategies are not mutually exclusive. In principle, it would be straightforward to incorporate both bulky terminal substituents and moderately electron-withdrawing groups onto an *o*-phenylene oligomer. Control of stacking interactions should, however, scale better for use in longer oligomers and polymers.

Because of the remarkable solvent dependence of the folding of **oP^n(FA)**, we wished to investigate the effect of solvent on the folding of our new oligomers. The NMR spectra of **oP^{10}(OAc)$_{10}$**^{A} in various solvents (benzene-d_6, chloroform-*d*, acetone-d_6, and acetonitrile-d_3) are shown in Figure 10. The

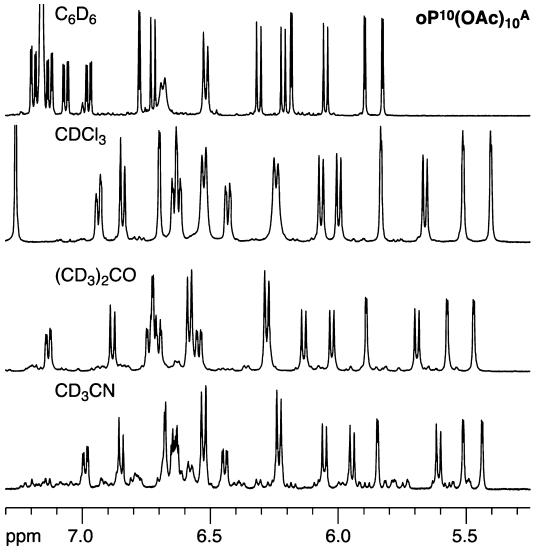

Figure 10. ^{1}H NMR spectra of **oP^{10}(OAc)$_{10}$**^{A} in benzene-d_6, chloroform-*d*, acetone-d_6, and acetonitrile-d_3 (500 MHz, rt).

oligomer folds well in all of the solvents examined, with near-perfect folding in benzene and chloroform. The worst folding is observed in acetonitrile, although the A_7 conformer still makes up ~75% of the total population. We also examined the solvent-dependence of the folding of **oP^6(CN)$_6$**^{A} (see Supporting Information). As in chloroform-*d*, we were unable to detect minor conformers in either acetone-d_6 or acetonitrile-d_3.

Taken together, the behavior of these two oligomers suggests that the improved folding we observe because of substituent effects is largely insensitive to solvent. It is noteworthy that the trend observed for **oP^{10}(OAc)$_{10}$**^{A}—weaker folding in more polar solvents—is the opposite of what has been reported for related systems based on aromatic stacking interactions. For example, Iverson has shown that stacking of a 1,5-dialkoxynaphthalene and a naphthalene dimide (both homo- and heterodimers), analogs of the structural units used in aedamers,[55] is strengthened by increasing solvent polarity because of the hydrophobic effect (i.e., desolvation of the aromatic faces on dimerization).[56] There are several key differences between this system and ours, however: Iverson observed the strongest effect for the formation of donor/acceptor heterodimers; the *o*-phenylenes considered here are analogous to homodimers. Acetonitrile, the most polar solvent considered in our study, is also not nearly as polar as many of the solvents they considered (water and methanol–water mixtures). It is also not clear that the solvation of an *o*-phenylene should be strongly dependent on its folding state, especially in comparison to Iverson's intermolecular systems. For the specific case of **oP^{10}(OAc)$_{10}$**^{A}, the total solvent effect on folding is sufficiently weak ($\Delta\Delta G^\circ \leq +0.7$ kcal/mol for acetonitrile vs chloroform) that it is possible it arises not from a direct effect on aromatic stacking, but rather from changes in other factors such as solvation.

Rapid Assessment of *o*-Phenylene Conformation. Despite its utility, the DFT/NMR method we use to characterize the folding states of *o*-phenylenes is admittedly time-consuming and challenging to apply to oligomers much longer than the [12]-mer. With a library of long, well-folded *o*-phenylenes in hand, it was possible to derive some empirical guidelines for judging the folding states of *o*-phenylene oligomers and polymers. In principle, it should be possible to apply these observations to other arene-rich architectures.

Looking at the overall set of ^{1}H NMR spectra of **oP^n(X)$_n$**^{A} and **oP^n(X)$_n$**^{B}, it is clear that the chemical shifts follow the same general trends regardless of the nature of the substituents and the particular substitution pattern, particularly at the upfield end of the aromatic region of the spectrum. In Figure 11, the backbone structure of **oP^{10}(OAc)$_{10}$**^{A} (from the crystal structure) is depicted with the aromatic protons colored according to their observed chemical shifts. As would be expected, the most shielded protons are those that are held close to the face of a nearby stacked ring. Protons in otherwise similar chemical environments show dramatically different

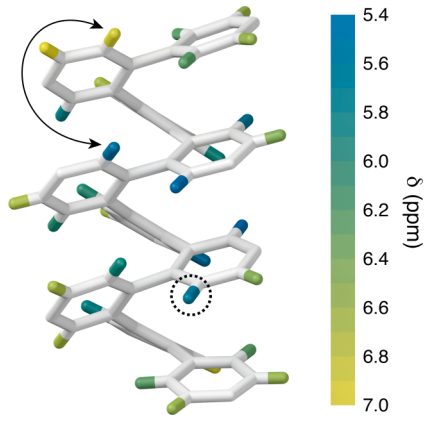

Figure 11. Experimental (solution) ^{1}H chemical shifts for **oP^{10}(OAc)$_{10}$**^{A}, drawn on its solid-state structure: The arrows highlight two protons in analogous positions but with very different chemical shifts. The circle highlights the proton that would be affected most if the end were misfolded. The acetate groups have been removed for clarity.

dx.doi.org/10.1021/ja509902m | J. Am. Chem. Soc. 2014, 136, 16666–16675

chemical shifts ($\Delta\delta \geq 1$ ppm) depending on their position within the helix. For example, the protons indicated by the arrows in Figure 11 would be expected to have similar chemical shifts, within ~0.3 ppm, on the basis of empirical substituent effects (one is *meta*, and the other *ortho* to an acetoxy group).[57] However, folding leads to a difference of 1.33 ppm, as one (bottom) is located directly beneath an aromatic ring in the folded structure. The circled proton in Figure 11 is a particularly sensitive reporter of the molecular conformation. Defects in *o*-phenylene folding tend to be localized at the oligomer ends[9] (as in the A_6B conformer). Should this occur, this proton is moved entirely out of the shielding zone of any arene. Consequently, the chemical shift difference for this proton between the AA...A and AA...B conformers is on the order of 1.3 ppm.

A second measure of the folding quality comes from UV−vis spectra as a function of length. Fukushima and Aida have previously proposed that minimal shifts in UV−vis absorbance with increasing length are an indicator of good folding in the *o*-phenylenes.[10] Thus, we were interested in the UV−vis spectra of our new homologous series of well-folded oligomers $\mathbf{oP^{\mathit{n}}(OAc)_{\mathit{n}}^{A}}$ and $\mathbf{oP^{\mathit{n}}(OTf)_{\mathit{n}}^{A}}$, and especially how they would compare with those of poorly folded $\mathbf{oP^{\mathit{n}}(H)_{\mathit{n}}}$ and $\mathbf{oP^{\mathit{n}}(OMe)_{\mathit{n}}^{A}}$. As shown in Figure 12, for both the acetoxy- and triflate-substituted oligomers, the (normalized) UV−vis spectra of the oligomers longer than the tetramer are essentially superimposable, with only a broad absorbance tapering off around 300 nm. Even at the extreme red edge of the spectra there are variations of only <3 nm from n = 4 to 10. This behavior contrasts with that of $\mathbf{oP^{\mathit{n}}(OMe)_{\mathit{n}}^{A}}$, for which a change of >8 nm was observed;[5] however, for the parent series $\mathbf{oP^{\mathit{n}}(H)_{\mathit{n}}}$, the change is similar (~3 nm). While this is obviously a small effect, it does suggest that small shifts in UV absorbance may be a useful indicator of good folding behavior in long *o*-phenylene oligomers and polymers when other data, such as NMR assignments, are difficult to obtain. However, this measure should be used cautiously, as the parent series also exhibits small changes in its UV−vis spectra[8] despite being the most poorly folded of the oligomers considered here.

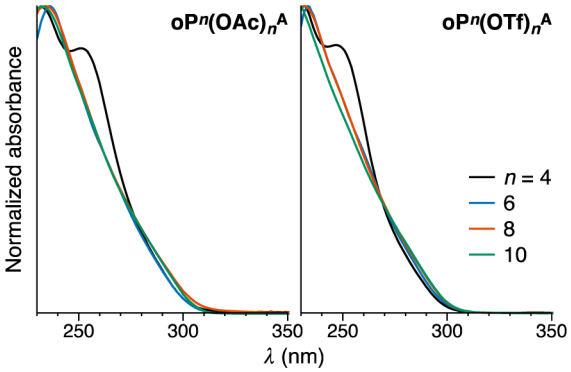

Figure 12. Normalized UV−vis spectra of $\mathbf{oP^{\mathit{n}}(OAc)_{\mathit{n}}^{A}}$ and $\mathbf{oP^{\mathit{n}}(OTf)_{\mathit{n}}^{A}}$ in CH_2Cl_2.

CONCLUSIONS

In summary, we have synthesized and characterized several new series of *o*-phenylene oligomers, incorporating increasingly electron-withdrawing substituents and varying the substitution pattern. In general, the use of even moderately electron-withdrawing substituents (i.e., acetoxy) gives substantially improved folding properties through the enhancement of intramolecular arene−arene stacking interactions. These effects can be modeled, to some extent, with PCM/B97-D/TZV-(2d,2p) calculations on small (tetramer) model compounds but are most easily rationalized using Hammett σ_m substituent constants. Oligomers up to the decamers have been investigated, with triflate functionalization giving essentially "perfect" folding in chloroform-*d*. The high-quality folding in these oligomers appears to be only weakly solvent-dependent. The principles developed here should be applicable to the design of other structurally congested polyphenylenes with well-defined three-dimensional structures.

EXPERIMENTAL SECTION

Unless otherwise noted, all starting materials, reagents, and solvents were purchased from commercial sources and used without further purification. Anhydrous tetrahydrofuran was obtained by distillation from sodium/benzophenone. Anhydrous dichloromethane was obtained by distillation from calcium hydride. NMR spectra were measured for chloroform-*d*, acetone-d_6, benzene-d_6, or acetonitrile-d_3 solutions using Bruker Avance 300 or 500 MHz NMR spectrometers. Temperature readings for low-temperature experiments (268 K) were calibrated using a 4% methanol in methanol-d_4 reference standard. Chemical shifts are reported in δ (ppm) relative to tetramethylsilane, with the residual solvent protons used as internal standards. UV−vis spectroscopy was performed using spectrometric-grade dichloromethane used without further purification. MMFF calculations were performed using *Spartan '08*,[58] PM7 calculations using *MOPAC2012*,[59] and DFT calculations using *Gaussian 09*.[60] Further details, including synthetic procedures, are included in the Supporting Information.

ASSOCIATED CONTENT

Supporting Information

Supplemental figures referred to in the text; NMR assignments and computational data (energies, geometries, GIAO calculations) for all new *o*-phenylene oligomers; crystal data for $\mathbf{oP^{6}(OMe)_{6}^{B}}$, $\mathbf{oP^{8}(OTf)_{8}^{A}}$, $\mathbf{oP^{10}(OAc)_{10}^{A}}$, and $\mathbf{oP^{10}(OTf)_{10}^{A}}$; experimental procedures; NMR spectra. This material is available free of charge via the Internet at http://pubs.acs.org.

AUTHOR INFORMATION

Corresponding Author

scott.hartley@miamioh.edu

Notes

The authors declare no competing financial interest.

ACKNOWLEDGMENTS

C.S.H. and S.M. acknowledge support from the National Science Foundation (CHE-1306437). C.J.Z. and L.A.C. acknowledge support from the University of Akron.

REFERENCES

(1) Wittig, G.; Lehmann, G. *Chem. Ber.* **1957**, *90*, 875−892.
(2) Kovacic, P.; Uchic, J. T.; Hsu, L.-C. *J. Polym. Sci., Part A-1: Polym. Chem.* **1967**, *5*, 945−964.
(3) Ozasa, S.; Fujioka, Y.; Fujiwara, M.; Ibuki, E. *Chem. Pharm. Bull.* **1980**, *28*, 3210−3222.
(4) Blake, A. J.; Cooke, P. A.; Doyle, K. J.; Gair, S.; Simpkins, N. S. *Tetrahedron Lett.* **1998**, *39*, 9093−9096.
(5) He, J.; Crase, J. L.; Wadumethrige, S. H.; Thakur, K.; Dai, L.; Zou, S.; Rathore, R.; Hartley, C. S. *J. Am. Chem. Soc.* **2010**, *132*, 13848−13857.

(6) Ohta, E.; Sato, H.; Ando, S.; Kosaka, A.; Fukushima, T.; Hashizume, D.; Yamasaki, M.; Hasegawa, K.; Muraoka, A.; Ushiyama, H.; Yamashita, K.; Aida, T. *Nat. Chem.* **2011**, *3*, 68−73.
(7) Hartley, C. S.; He, J. *J. Org. Chem.* **2010**, *75*, 8627−8636.
(8) Mathew, S. M.; Hartley, C. S. *Macromolecules* **2011**, *44*, 8425−8432.
(9) Mathew, S. M.; Engle, J. T.; Ziegler, C. J.; Hartley, C. S. *J. Am. Chem. Soc.* **2013**, *135*, 6714−6722.
(10) Ando, S.; Ohta, E.; Kosaka, A.; Hashizume, D.; Koshino, H.; Fukushima, T.; Aida, T. *J. Am. Chem. Soc.* **2012**, *134*, 11084−11087.
(11) Kajitani, T.; Suna, Y.; Kosaka, A.; Osawa, T.; Fujikawa, S.; Takata, M.; Fukushima, T.; Aida, T. *J. Am. Chem. Soc.* **2013**, *135*, 14564−14567.
(12) Berresheim, A. J.; Müller, M.; Müllen, K. *Chem. Rev.* **1999**, *99*, 1747−1785.
(13) Grimsdale, A. C.; Müllen, K. *Adv. Polym. Sci.* **2006**, *199*, 1−82.
(14) Kandre, R.; Feldman, K.; Meijer, H. E. H.; Smith, P.; Schlüter, A. D. *Angew. Chem., Int. Ed.* **2007**, *46*, 4956−4959.
(15) Reddinger, J. L.; Reynolds, J. R. *Macromolecules* **1997**, *30*, 479−481.
(16) Ben, T.; Goto, H.; Miwa, K.; Goto, H.; Morino, K.; Furusho, Y.; Yashima, E. *Macromolecules* **2008**, *41*, 4506−4509.
(17) Miwa, K.; Furusho, Y.; Yashima, E. *Nat. Chem.* **2010**, *2*, 444−449.
(18) Goto, H.; Furusho, Y.; Yashima, E. *J. Am. Chem. Soc.* **2007**, *129*, 9168−9174.
(19) Pisula, W.; Kastler, M.; Yang, C.; Enkelmann, V.; Müllen, K. *Chem.—Asian. J.* **2007**, *2*, 51−56.
(20) Schwab, M. G.; Qin, T.; Pisula, W.; Mavrinskiy, A.; Feng, X.; Baumgarten, M.; Kim, H.; Laquai, F.; Schuh, S.; Trattnig, R.; List, E. J. W.; Müllen, K. *Chem.—Asian. J.* **2011**, *6*, 3001−3010.
(21) Golling, F. E.; Quernheim, M.; Wagner, M.; Nishiuchi, T.; Müllen, K. *Angew. Chem., Int. Ed.* **2014**, *53*, 1525−1528.
(22) Omachi, H.; Segawa, Y.; Itami, K. *Acc. Chem. Res.* **2012**, *45*, 1378−1389.
(23) Evans, P. J.; Darzi, E. R.; Jasti, R. *Nat. Chem.* **2014**, *6*, 404−408.
(24) Bauer, R. E.; Grimsdale, A. C.; Müllen, K. *Top. Curr. Chem.* **2005**, *245*, 253−286.
(25) Gellman, S. H. *Acc. Chem. Res.* **1998**, *31*, 173−180.
(26) Hill, D. J.; Mio, M. J.; Prince, R. B.; Hughes, T. S.; Moore, J. S. *Chem. Rev.* **2001**, *101*, 3893−4011.
(27) Guichard, G.; Huc, I. *Chem. Commun.* **2011**, *47*, 5933−5941.
(28) Arslan, H.; Saathoff, J. D.; Bunck, D. N.; Clancy, P.; Dichtel, W. R. *Angew. Chem., Int. Ed.* **2012**, *51*, 12051−12054.
(29) Manabe, K.; Kimura, T. *Org. Lett.* **2013**, *15*, 374−377.
(30) Yamaguchi, M.; Kimura, T.; Shinohara, N.; Manabe, K. *Molecules* **2013**, *18*, 15207−15219.
(31) Lee, D. R.; Lee, C. W.; Lee, J. Y. *J. Mater. Chem. C* **2014**, *2*, 7256−7263.
(32) Ito, S.; Takahashi, K.; Nozaki, K. *J. Am. Chem. Soc.* **2014**, *136*, 7547−7550.
(33) Yashima, E.; Maeda, K.; Iida, H.; Furusho, Y.; Nagai, K. *Chem. Rev.* **2009**, *109*, 6102−6211.
(34) These distances are estimated from a B97-D/TZV(2d,2p) geometry optimization of the perfectly folded parent dodecamer.
(35) Wheeler, S. E. *J. Am. Chem. Soc.* **2011**, *133*, 10262−10274.
(36) Ishikawa, S.; Manabe, K. *Chem. Lett.* **2006**, *35*, 164−165.
(37) Carson, M. W.; Giese, M. W.; Coghlan, M. J. *Org. Lett.* **2008**, *10*, 2701−2704.
(38) Al-Zoubi, R. M.; Hall, D. G. *Org. Lett.* **2010**, *12*, 2480−2483.
(39) A notable exception to the inertness of the backbone is the potential for rearrangements under acidic or oxidative conditions; see: Ajaz, A.; McLaughlin, E. C.; Skraba, S. L.; Thamatam, R.; Johnson, R. P. *J. Org. Chem.* **2012**, *77*, 9487−9495.
(40) Ito, Y.; Miyake, T.; Hatano, S.; Shima, R.; Ohara, T.; Suginome, M. *J. Am. Chem. Soc.* **1998**, *120*, 11880−11893.
(41) Nagata, Y.; Takagi, K.; Suginome, M. *J. Am. Chem. Soc.* **2014**, *136*, 9858−9861.
(42) Quantification was done at 268 K to take advantage of a slight sharpening of the signals. The spectra at rt are very similar in appearance.
(43) Stewart, J. J. P. *J. Mol. Model.* **2012**, *19*, 1−32.
(44) Grimme, S. *J. Comput. Chem.* **2006**, *27*, 1787−1799.
(45) Wiitala, K. W.; Hoye, T. R.; Cramer, C. J. *J. Chem. Theory Comput.* **2006**, *2*, 1085−1092.
(46) Jain, R.; Bally, T.; Rablen, P. R. *J. Org. Chem.* **2009**, *74*, 4017−4023.
(47) Obviously, the AAB conformer does not conform to the symmetry of the (2-fold symmetric) experimentally observed conformer. It was chosen as one of the test cases because it has always been the second-most populated conformer in previous systems and serves as a useful stand-in for an arbitrary conformational state.
(48) Note that this definition of ΔG°_{fold} is slightly different from the one used in ref 9.
(49) Hansch, C.; Leo, A.; Taft, R. W. *Chem. Rev.* **1991**, *91*, 165−195.
(50) Cozzi, F.; Cinquini, M.; Annuziata, R.; Siegel, J. S. *J. Am. Chem. Soc.* **1993**, *115*, 5330−5331.
(51) Cockroft, S. L.; Hunter, C. A.; Lawson, K. R.; Perkins, J.; Urch, C. J. *J. Am. Chem. Soc.* **2005**, *127*, 8594−8595.
(52) Fischer, F. R.; Schweizer, W. B.; Diederich, F. *Chem. Commun.* **2008**, 4031−4033.
(53) Seo, J.-I.; Kim, I.; Lee, Y. S. *Chem. Phys. Lett.* **2009**, *474*, 101−106.
(54) For the methoxy substituents, 2-fold permutations were considered. For acetoxy substituents, we considered 4-fold permutations about the arene−O bond. For triflate, we considered all possible 4-fold permutations about the arene−O bond and 3-fold permutations about the O−S bond.
(55) Lokey, R. S.; Iverson, B. L. *Nature* **1995**, *375*, 303−305.
(56) Cubberley, M. S.; Iverson, B. L. *J. Am. Chem. Soc.* **2001**, *123*, 7560−7563.
(57) Silverstein, R. M.; Webster, F. X.; Kiemle, D. J. *Spectrometric Identification of Organic Compounds*, 7th ed.; John Wiley & Sons, Inc.: New York, 2005.
(58) *Spartan '08*, Ver. 1.2.0; Wavefunction, Inc.: Irvine, CA, 2006.
(59) Stewart, J. J. P. *MOPAC2012*, Ver. 14.014M; Stewart Computational Chemistry: Colorado Springs, CO, 2012.
(60) Frisch, M. J.; Trucks, G. W.; Schlegel, H. B.; Scuseria, G. E.; Robb, M. A.; Cheeseman, J. R.; Scalmani, G.; Barone, V.; Mennucci, B.; Petersson, G. A.; Nakatsuji, H.; Caricato, M.; Li, X.; Hratchian, H. P.; Izmaylov, A. F.; Bloino, J.; Zheng, G.; Sonnenberg, J. L.; Hada, M.; Ehara, M.; Toyota, K.; Fukuda, R.; Hasegawa, J.; Ishida, M.; Nakajima, T.; Honda, Y.; Kitao, O.; Nakai, H.; Vreven, T.; Montgomery, J. A., Jr.; Peralta, J. E.; Ogliaro, F.; Bearpark, M.; Heyd, J. J.; Brothers, E.; Kudin, K. N.; Staroverov, V. N.; Keith, T.; Kobayashi, R.; Normand, J.; Raghavachari, K.; Rendell, A.; Burant, J. C.; Iyengar, S. S.; Tomasi, J.; Cossi, M.; Rega, N.; Millam, J. M.; Klene, M.; Knox, J. E.; Cross, J. B.; Bakken, V.; Adamo, C.; Jaramillo, J.; Gomperts, R.; Stratmann, R. E.; Yazyev, O.; Austin, A. J.; Cammi, R.; Pomelli, C.; Ochterski, J. W.; Martin, R. L.; Morokuma, K.; Zakrzewski, V. G.; Voth, G. A.; Salvador, P.; Dannenberg, J. J.; Dapprich, S.; Daniels, A. D.; Farkas, O.; Foresman, J. B.; Ortiz, J. V.; Cioslowski, J.; Fox, D. J. *Gaussian 09*, Rev. B.01; Gaussian, Inc.: Wallingford, CT, 2010.